Dyes and Pigments 15 (1991) 139–156

Organic Photoconductive (OPC) Devices Incorporating Bisarylimidazole Perinone Pigments

R. O. Loutfy, A. M. Hor,* P. M. Kazmaier,
R. A. Burt & G. K. Hamer

Xerox Research Centre of Canada,
2660 Speakman Drive, Mississauga, Ontario, Canada L5K 2L1

(Received 15 March 1990; accepted 25 April 1990)

ABSTRACT

The synthesis and purification of a series of four bisarylimidazole perinone photoconductive pigments is described. The optical and electrical properties of negatively charged dual-layer photoreceptors incorporating a thin 0·20 μm evaporated film of the bisarylimidazole perinones and a thick (15 μm) hole transport layer were determined. The photoreceptor devices exhibit low dark decay, excellent cyclic stability and high white light photosensitivity. An improvement in the spectral response above 600 nm was obtained by varying the chemical structure of the perinone.

INTRODUCTION

The perinone pigments investigated in this work are bisarylimidazole derivatives of naphthalene-1,4,5,8-tetracarboxylic acid and are formed by the condensation of aromatic diamines with the acid or acid anhydride. The reaction product is a mixture of the *cis* and *trans* isomers of the perinone (see Scheme 1). Perinones are a class of orange-to-red pigments which exhibit excellent lightfastness, good bleed, bake and chemical resistance, transparency and moderate color intensity. They are widely used as colorants in plastics, printing inks and metallic automotive paints. The uses of perinones as photogenerators with polyvinylcarbazole (PVK) as the charge transport layer in photoreceptor devices have been reported.[1,2]

* Author to whom correspondence should be addressed.

Dyes and Pigments 0143-7208/91/$03·50

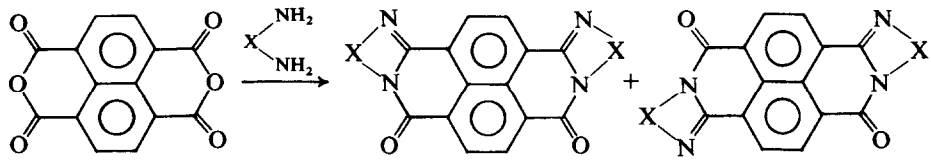

Scheme 1. Synthesis of bisarylimidazole perinones.

In the present study, we have investigated the photoconductive (xerographic) behaviour of thin evaporated films of bisarylimidazole perinone compounds. In particular, we attempted to establish the relationship between the molecular structure of these pigments and their photoactivity. Additional objectives of the work were to extend the spectral response of perinone derivatives to wavelengths above 600 nm and to examine the effects of charge transport materials on xerographic performance.

EXPERIMENTAL

Materials

Four bisarylimidazole perinones, the structures of which are shown in Scheme 2, were synthesized by reacting naphthalene-1,4,5,8-tetracarboxylic acid dianhydride with the appropriate aromatic diamine in 1-chloronaphthalene or acetic acid. Products were purified by temperature gradient sublimation.[3] Alternatively, purified perinones were prepared from commercial materials as follows.

Isolation of *cis*-bis(benzimidazole) perinone, 1

Purified *cis*-bis(benzimidazole) perinone was isolated by diluting 40 ml of Hoechst Vat Red 15 ink to 600 ml with methanol and centrifuging at 10 000 rpm. The precipitate formed was separated from the supernatant liquor and dried (9·55 g). Figure 1 shows the UV–visible absorption spectrum of the resulting pigment in sulfuric acid, with strong absorption maxima at 484 and 377 nm.

Isolation of *trans*-bis(benzimidazole) perinone, 2

Purified *trans*-bis(benzimidazole) perinone was isolated by filtration of 40 ml Hoechst Vat Orange 7 ink through a 0·5 μm PTFE® filter. The resulting

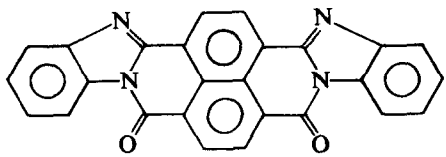

1

Cis-Bis(benzimidazole) perinone

Indanthrene Bordeaux (Vat Red 15)

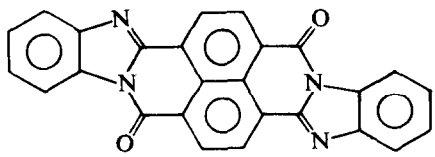

2

Trans-Bis(benzimidazole) perinone

Indanthrene Brilliant Orange (Vat Red 7)

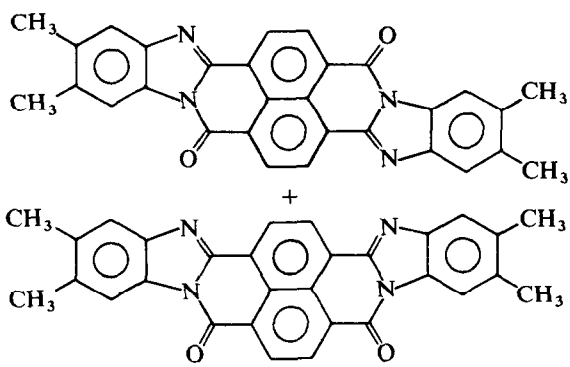

3

Trans- and *Cis*-Bis(4,5-dimethylbenzimidazole) perinone

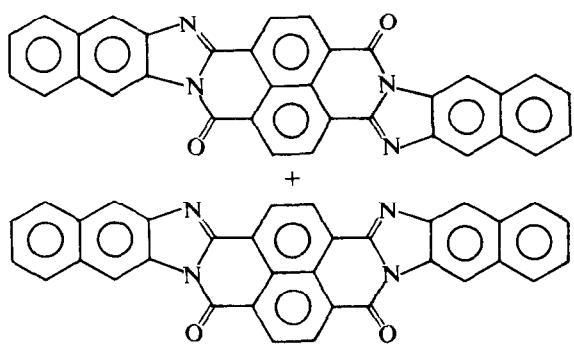

4

Trans- and *Cis*-Bis(2,3-naphthimidazole) perinone

Scheme 2. Chemical structures of bisarylimidazole perinones.

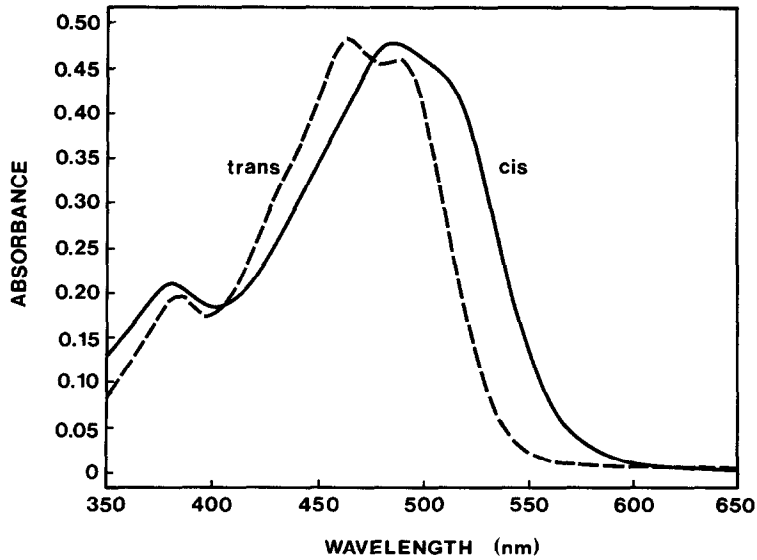

Fig. 1. The absorption spectra of *cis*- and *trans*-bis(benzimidazole) perinone, **1** and **2** respectively, in H_2SO_4 solution.

precipitate was washed twice with methanol and dried at 110°C for 4 h (5·3 g isolated). Figure 1 shows the UV–visible absorption spectrum in sulfuric acid of the resulting product, with strong maxima at 486, 464 and 384 nm.

Spectroscopic characterization of *cis*- and *trans*-bis(benzimidazole) perinone, 1 and 2

Figure 2 shows the FTIR spectra of the *cis*- and *trans*-bis(benzimidazole) perinone, **1** and **2** respectively, taken in the diffuse reflectance mode. The two spectra are very similar, except that many of the absorption peaks observed for the *trans* isomer appear as doublets for the *cis* isomer. Carbon-13 CP/MAS solid-state NMR spectra of **1** and **2** are shown in Fig. 3. Again there is great similarity between the two spectra except for the region below 130 ppm.

Solution ^{1}H-NMR spectra of *cis*- and *trans*-bis(benzimidazole) perinone, **1** and **2**, recorded at 250 MHz in trifluoroacetic acid (TFA) are shown in Fig. 4. The naphthalene ring protons of the *cis* isomer are expected to give rise to two resonances, with no interproton coupling. The *trans* isomer, on the other hand, is expected to display an $[AB]_2$ for the naphthalene ring protons, consisting of four absorption lines. These expected patterns are observed (Fig. 4), although the chemical shift dispersion at 250 MHz is slight. In an attempt to increase the dispersion range, deuterated benzene (C_6D_6) solvent-induced shifts were investigated. Figure 5(a) and (b) shows the effect of

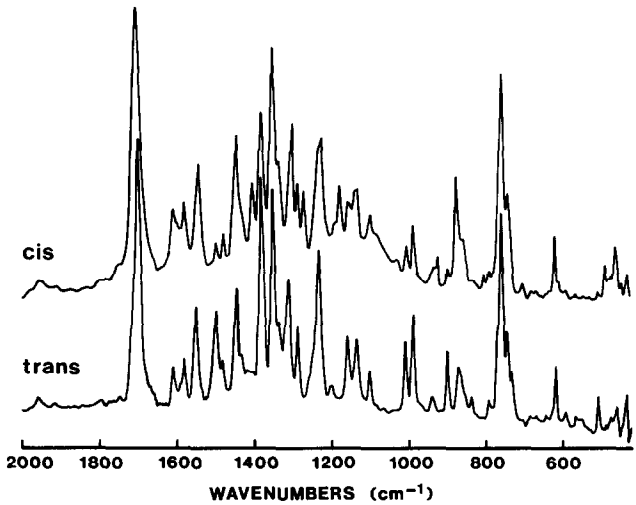

Fig. 2. The FTIR spectra of **1** and **2**.

different C_6D_6/TFA solvent compositions on the ^1H chemical shifts of the naphthalene ring protons of **1** and **2** respectively. At 1:1 volume ratio of C_6D_6/TFA, the spectrum of the *cis* isomer shows two well-separated resonances (one sharp, the other very broad) but, in addition, the four-line pattern due to the *trans* isomer. Integration of this spectrum indicates that the *cis*-bis(benzimidazole) perinone sample is in fact contaminated with the *trans* isomer to the extent of 15%. In contrast, the ^1H-NMR spectrum of

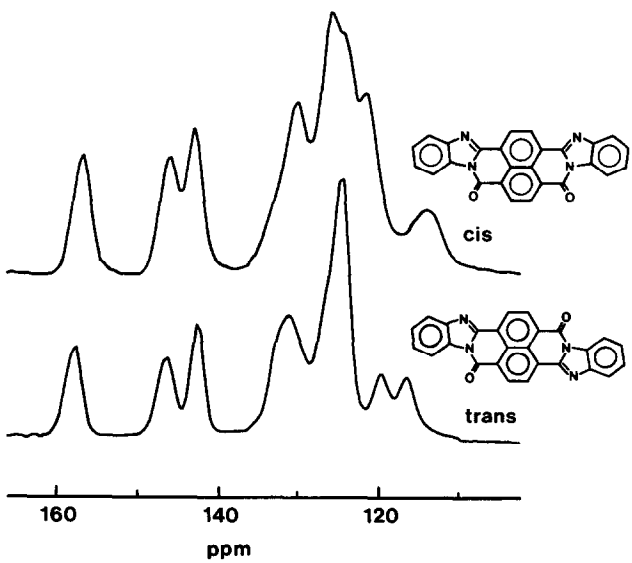

Fig. 3. The solid-state ^{13}C-NMR spectra of **1** and **2**.

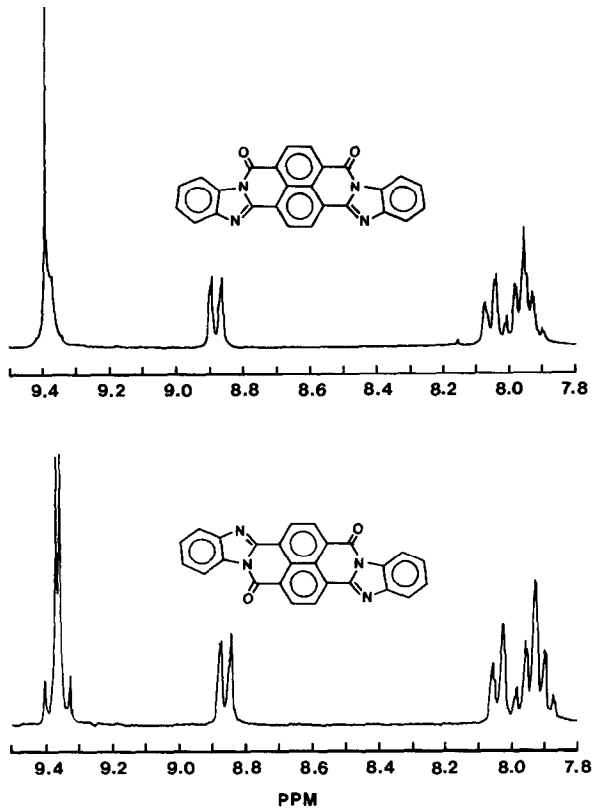

Fig. 4. The solution NMR spectra of **1** and **2** in TFA.

trans-bis(benzimidazole) perinone in C_6D_6:TFA (1:1) shows only the $[AB]_2$ pattern with no trace of *cis* isomer resonances, i.e. the *trans* isomer is 100% pure.

Synthesis of bis(4,5-dimethylbenzimidazole) perinone, 3

A mixture of naphthalene-1,4,5,8-tetracarboxylic acid dianhydride (13·41 g, 0·050 mol), 4,5-dimethyl *o*-phenylenediamine (34·1 g, 0·250 mol) and 1-chloronaphthalene (250 ml) was heated to 250°C for 2 h (under nitrogen), after which the visible absorption spectrum indicated that the reaction was complete. The resulting product was isolated by filtration, and purification was accomplished by slurrying the product in toluene at 90°C for 1 h and filtering. The aforementioned slurry–filter cycle was repeated three times. Thereafter, the product was dried at 95°C at 260 torr overnight. Yield was 95·6%.

The UV–visible absorption of the above product in sulfuric acid showed a maximum at 534 nm ($\varepsilon = 26\,610$), and the IR spectrum evidenced a typical

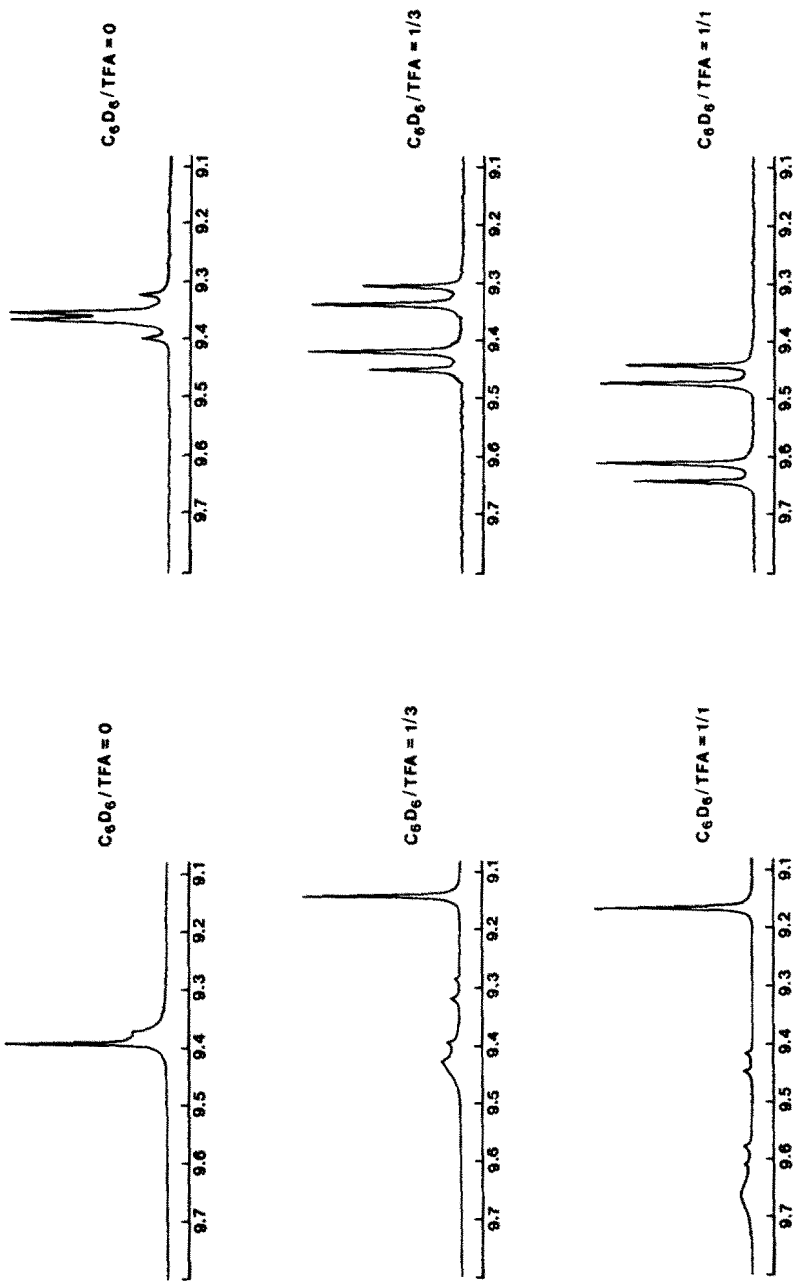

Fig. 5. The effect of adding C_6D_6 on the solution NMR spectra of (a) **1** and (b) **2** in TFA.

perinone imidazole band at 1697 cm^{-1}. The mass spectrum indicated a molecular ion at m/z 468.

Combustion analysis. Calcd: C, 76·91; H, 4·30; N, 11·96. Found: C, 76·81; H, 4·32; N, 11·99%.

Synthesis of bis(2,3-naphthimidazole) perinone, 4

A mixture of naphthalene-1,4,5,8-tetracarboxylic acid dianhydride (4·24 g, 15·8 mmol) and 2,3-diaminonaphthalene (5·0 g, 31·6 mmol) in acetic acid (25 ml) was heated slowly to reflux (1·5 h) and refluxed for 5 h. TLC indicated that all of the diaminonaphthalene had reacted to form the corresponding bisimide after 1 h. Cyclization proceeded slowly during the reflux period and ceased after about 50% of the bisimide had cyclized (estimated from the IR spectrum). The product was isolated by filtration (0·5 μm PTFE® filter), and was solvent-purified by: (1) boiling with acetic acid (300 ml) for 15 min, followed by filtration; (2) boiling with acetic acid (50 ml) for 4 h, followed by filtration. A portion of the product (3·98 g) was then train-sublimed at 0·1 torr/487°C.[3] The yield of naphthimidazole perinone recovered was 42·5% (1·69 g). A molecular ion at m/z 512 was observed and the IR spectrum indicated the presence of the perinone imidazole band.

Since the intent of this work was to explore the potential of evaporated films of bisarylimidazole perinones as charge generators in photoreceptors, the preparation of evaporated films and their characteristics is therefore described in detail.

Preparation of evaporated films of bisarylimidazole perinones

Thin films of perinones in thicknesses ranging from 200–400 nm were prepared by vacuum evaporation in a Balzers BAE020 coater. Among various evaporation sources used, the tantalum boat (Part ME 2/2B, purchased from R. D. Mathis) was found most satisfactory. During the course of evaporation the system base pressure was stable at $<10^{-5}$ torr. The rate of deposition was maintained between 0·2–0·4 nm s^{-1}, as monitored by an Inficon thickness monitor. The substrate was either a Corning glass slide or aluminized Mylar overcoated with a polyester adhesive layer 0·1 μm thick.

Optical absorption of evaporated films

The optical absorption spectra of thin (200 nm) evaporated films of bisarylimidazole perinones **1**–**4** deposited onto a glass slide are shown in Fig. 6. The solid-state absorption maxima for the evaporated perinone films are

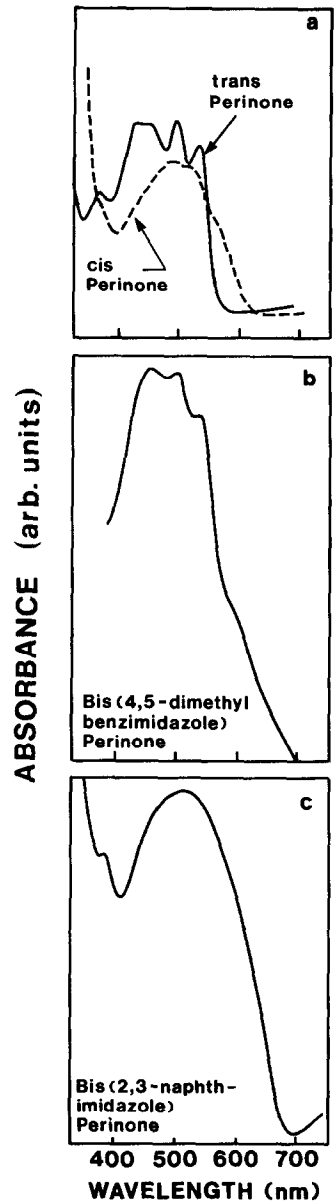

Fig. 6. The solid-state absorption spectra of 0·2 μm evaporated films of (a) **1** and **2**, (b) **3** and (c) **4**.

TABLE 1

Chemical Structures, Solid-State Absorption and Xerographic Data for Bisarylimidazole Perinones

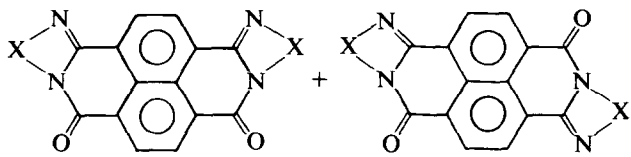

Bisarylimidazole perinone

	X	Solid state, λ_{max} (nm)	Xerographic data[a]			
			Dark decay ($V s^{-1}$)	$E_{1/2}$ (erg cm^{-2})		Discharge at 10 erg cm^{-2}, 400–700 nm (%)
				$\lambda_{400-700}$	λ_{max}	
1	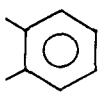 (*cis* + 15% *trans*)	450(S), 485, 520, 570(S)	3–6	10	3·3	50
2	 (*trans* only)	450, 495, 530	2–7	12	3·3	47
3	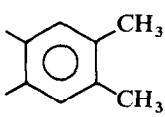	460, 500, 538, 600(S)	7–10	8·8	2·8	60
4	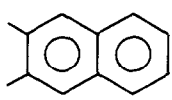	515, 610(S)	8–10	9·2	5·7	53

[a] 0·2 μm CGL. 15 μm CTL of 35% TPD/Merlon.

given in Table 1. It is interesting to note that the absorption maximum of the *cis*-bis(benzimidazole) perinone is slightly red-shifted compared with that of the *trans* isomer but is less structured. Both the bis(4,5-dimethylbenzimidazole) perinone (**3**) and bis(2,3-naphthimidazole) perinone (**4**) exhibit significant absorption beyond 600 nm, as shown in Figs 6(b) and (c).

Photoreceptor device fabrication

The photoreceptor device configuration used to evaluate the bisarylimidazole perinones **1–4** was a dual-layer structure, as shown in Fig. 7. The substrate was a 75-micron aluminized Mylar sheet overcoated with a thin

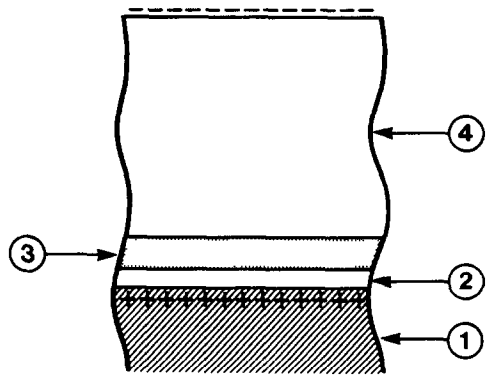

1. Conductive substrate
2. Charge blocking layer and adhesive layer
3. Charge generation layer
4. Charge transport layer

Fig. 7. The cross-section of a dual-layer photoreceptor.

0·03 μm silane charge blocking layer and a 0·1 μm polyester adhesive layer. The charge generator layer (CGL) was a thin 0·2 μm evaporated film of perinone pigment. The charge transport layer (CTL) comprised 35 wt% *N,N'*-diphenyl-*N,N'*-bis(3-methylphenyl)-[1,1'-bisphenyl]-4,4'-diamine (TPD) in bisphenol-A-polycarbonate (Merlon), or as otherwise stated. The charge transport layer was coated from the dichloromethane solution using a modified Gardner mechanical-drive film coater. The sample was dried in a forced air oven at a temperature of about 135°C for 20 min to produce an approximately 15 ± 1 μm-thick hole transport layer.

Xerographic measurement

Xerographic discharge measurements were carried out using a computer-controlled xerographic cycling system. The samples were mounted onto the flat-plate scanner. A wire-corotron was used for charging the samples. The surface potential was measured using a wire loop connected to a Keithley 616 electrometer. The first surface potential reading (V_0) was measured 0·31 s after charging. After another 0·5 s, the dark development potential (V_{DDP}) was measured and photodischarge was then initiated by a 20-ms light pulse. The light source was a 150W xenon lamp and both broadband white light (400–700 nm) and monochromatic light illuminations were produced by using appropriate filters. Exposure and erasure energies were measured using a Karl Lambrecht dc 1010 lightmeter. This lightmeter was equipped

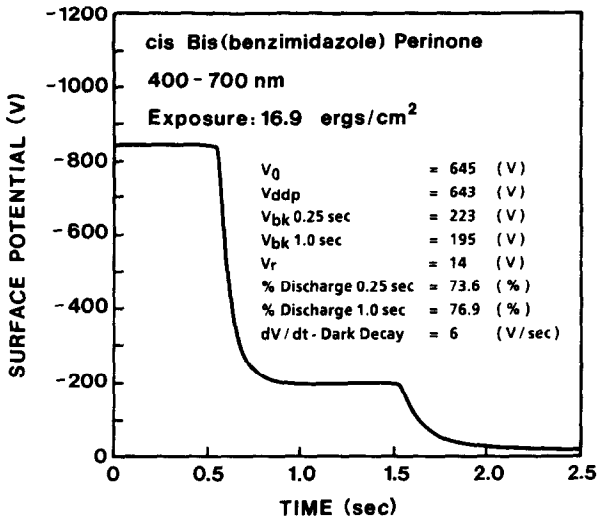

Fig. 8. Xerographic single discharge curve for photoreceptor incorporating perinone 1.

with a P1111 light probe which has a near-flat irradiance response from 400 to 1000 nm. The dark development potential (V_{DDP}) was always kept at −800 V and the dark decay was calculated from the data points taken between V_0 and V_{DDP}. The variation of surface potential with time after the exposure was measured; the term background potential (V_{BK}) is commonly used to refer to the surface potential after exposure. The photoreceptor was then erased with a light 15 times more intense than the exposure light to

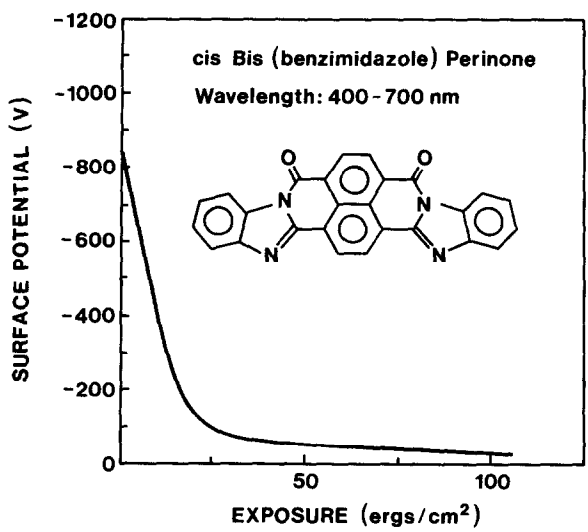

Fig. 9. Xerographic photoinduced discharge curve (PIDC) for a dual-layer photoreceptor incorporating compound 1.

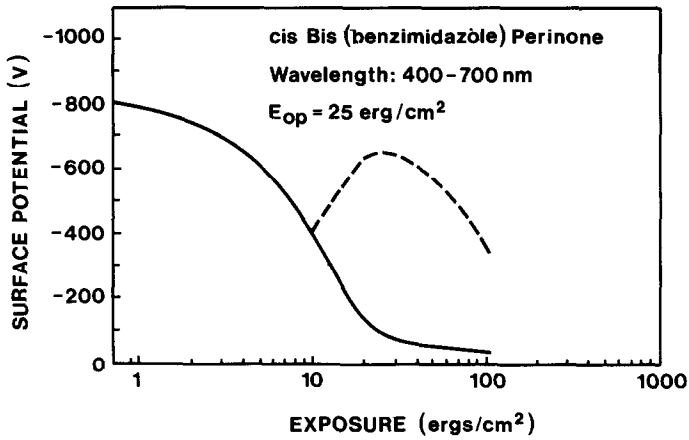

Fig. 10. Xerographic surface-potential versus exposure (——) and contrast potential (– – –) curves for a dual-layer photoreceptor incorporating compound **1**.

produce a second photodischarge, resulting in a further drop in surface potential to a value called the residual potential (V_R).

Figure 8 shows a typical single discharge curve (time-resolved surface potential measurement) of a dual-layer photoreceptor device that incorporates a thin (0·2 μm) film of compound **1**. The photoinduced discharge curves (PIDCs) were obtained by performing a number of single discharge curve experiments at varying exposures. From these single discharge curves the surface potential at a given time (0·25 s) after exposure was plotted against exposure energy. A typical PIDC for a dual-layer photoreceptor incorporating an evaporated film of pigment is shown in Fig. 9. From the PIDC curve, $E_{1/2}$, the exposure energy (in erg cm^{-2}) required to reduce the surface potential V_{DDP} to half of its initial value was determined. The higher the photosensitivity, the smaller is the exposure energy required to discharge the photoreceptor device to 50% of the initial surface potential. In Table 1, the dark decay in V s^{-1} and the photosensitivity $E_{1/2}$ in erg cm^{-2} of negatively charged dual-layer photoreceptors incorporating thin evaporated films (0·2 μm) of the perinone pigments **1** to **4** are given. Figure 10 shows a plot of surface potential versus log exposure, and also the contrast potential curve for a dual-layer photoreceptor incorporating an evaporated film of pigment **1**. The optimum exposure (E_{OP}) at an input optical density of 1·0 can be determined from the peak of the contrast potential curve.

The xerographic cyclic behavior of several dual-layer photoreceptors made with different perinone generator materials was determined by cycling each device through the charge–discharge–erase cycles for several thousand times and measuring V_0, V_{DDP}, V_{BK} at 1·0 and 1·7 s after exposure and V_R, the residual potential, after erasure for each cycle. Figure 11 shows the results

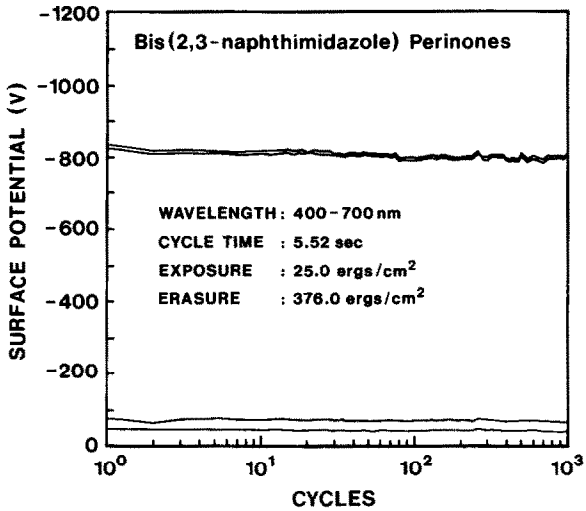

Fig. 11. Xerographic cyclic stability plot for a dual-layer photoreceptor incorporating compound **4**.

for a dual-layer photoreceptor incorporating an evaporated film of compound **4**.

The spectral sensitivity response of the dual-layer photoreceptors incorporating perinone pigments was measured by determining the exposure required to reduce the surface potential from −800 to −400 V, i.e. $E_{1/2}$ at different wavelengths from 400 to 900 nm. Results are illustrated in Fig. 12, where the inverse of $E_{1/2}$ is plotted against wavelength.

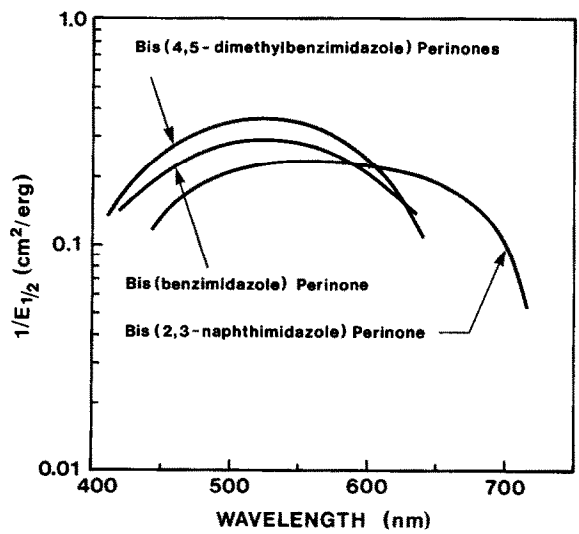

Fig. 12. The spectral response curves ($1/E_{1/2}$ versus wavelength) for dual-layer photoreceptors incorporating compounds (a) **1**, (b) **2** and (c) **4** as a 0·2 μm evaporated CGL.

RESULTS AND DISCUSSION

The use of certain bisarylimidazole perinones and thiazinobenzimidazole perinones as photogenerator pigments in electrophotographic devices is known.[1,2] However, the photoinjection of holes from these perinones has been studied only with polyvinylcarbazole (PVK) as charge transport layer. Furthermore, the spectral response of these perinones was limited to wavelengths shorter than 600 nm. We have investigated the xerographic performance of several bisarylimidazole perinones with PVK and other hole-transporting materials. The chemical structures of our perinones were chosen to give broader absorption and spectral shifts beyond 600 nm. Establishing the relationship between the molecular structure of bisarylimidazole perinones and their photoactivity was also one of our objectives. Table 1 summarizes the xerographic performance data for the bisarylimidazole perinones studied, using TPD/Merlon as a charge transport layer. The bis(4,5-dimethylbenzimidazole) perinone **3** exhibits the highest monochromatic photosensitivity ($E_{1/2}$ at λ_{max} 525 nm = 2·8 erg cm^{-2}), while the parent *cis*- or *trans*-bisbenzimidazole perinone **1** or **2** exhibits an $E_{1/2}$ at λ_{max} 525 nm of 3·3 erg cm^{-2}, i.e. 17% lower than the dimethyl derivative. The bis(2,3-naphthimidazole) perinone **4** exhibits the lowest monochromatic photosensitivity in the series with $E_{1/2}$ at λ_{max} = 5·7 erg cm^{-2}, i.e. 46% lower than bis(4,5-dimethylbenzimidazole) perinone **3**. The white light (λ = 400–700 nm) photosensitivity of the bis(4,5-dimethylbenzimidazole) perinone **3** is still the highest with $E_{1/2}$ of 8·8 erg cm^{-2}, but the bis(2,3-naphthimidazole) perinone **4** has a higher white light photosensitivity ($E_{1/2}$ = 9·2 erg cm^{-2}) than the bisbenzimidazole perinones **1** or **2** ($E_{1/2}$ = 10 and 12 erg cm^{-2} respectively). The enhancement of the white light photosensitivity of **4** compared with **1** and **2** is due to the fact that **4** has a broader and red-shifted absorption spectrum and thus absorbs more of the white light. The dark decays of perinone devices are very low and their cyclic stabilities are excellent (see Fig. 11).

Effect of the charge-transport-layer materials on bisarylimidazole perinone photoreceptor performance

The dependence of the xerographic electricals of bisbenzimidazole perinone **1** and bis(2,3-naphthimidazole) perinone **4** on the type of the charge-transport-layer materials was investigated using PVK and a solid solution of TPD in Merlon. Table 2 summarizes the xerographic data for negatively charged dual-layer photoreceptor devices incorporating a 0·2 μm CGL of evaporated film of **1** and **4** with a 15 μm CTL of PVK or TPD/Merlon. It is quite clear that the choice of the CTL materials has a significant influence on

TABLE 2

Effect of Charge Transport Layer (CTL) on the Xerographic Performance of Bis(benzimidazole) and Bis(2,3-naphthimidazole) Perinone Photoreceptor Devices[a]

CTL	*CGL*					
	Bis(benzimidazole) perinone **1**			*Bis(2,3-naphthimidazole) perinone* **4**		
	Dark decay ($V s^{-1}$)	$E_{1/2}$ ($erg\ cm^{-2}$)	*Discharge at* $10\ erg\ cm^{-2}$ (%)	*Dark decay* ($V s^{-1}$)	$E_{1/2}$ ($erg\ cm^{-2}$)	*Discharge at* $10\ erg\ cm^{-2}$ (%)
PVK	3	31	18	6	174	5
35% TPD in Merlon	5	10	50	16	10	50

[a] CGL thickness, 0·2 μm; CTL thickness, 15 μm; $\lambda = 400$–700 nm.

the photosensitivity of the devices. The photosensitivity of the bis(benzimidazole) perinone **1** increases by a factor of 3 on switching from PVK to TPD/Merlon as charge transport layer. Similarly, the photosensitivity of the bis(2,3-naphthimidazole) perinone P/R device increases by more than an order of magnitude by changing the CTL from PVK to TPD/Merlon. Generally speaking, the photosensitivity of a negatively charged dual-layer photoreceptor depends on several factors, viz. carrier generation in CGL, hole injection from CGL into CTL and transport properties of CTL. For the perinone photoreceptors, all these factors are more favored with the TPD/Merlon CTL than with the PVK. The photogeneration process in perinone photoreceptors probably belongs to the surface sensitization mechanism which has been observed for a similar polycyclic compound, namely benzimidazole perylene.[4] The dissociation of photogenerated excitons into free carriers which takes place at the CGL/CTL interface is greatly facilitated by an electron donor in CTL capable of injecting electrons into the excited pigment. The net result is holes injected from the CGL into the CTL, which then move across the CTL to neutralize the negative surface charges. Electrochemical measurement indicated that for molecules in solution PVK has a relatively high oxidation potential ($E_{1/2}$, ox = 1·4 V vs SCE) compared with TPD ($E_{1/2}$, ox = 0·85 V vs SCE). Qualitatively, in the solid state, PVK has a higher ionization potential than TPD and hence is a poorer electron donor. Fluorescence measurement[6] revealed that TPD effectively quenched the fluorescence of perinones whereas PVK had very little effect. These experimental observations suggest that the energy level of the excited pigment to receive an injected electron from a donor lies below the HOMO (highest occupied molecular) level of TPD, but above that of PVK. As a result, the surface-sensitized photogeneration of carriers, as well

TABLE 3
Effect of Charge Generator Layer (CGL) Thickness on the Xerographic Performance of Bis(2,3-naphthimidazole) Perinone Photoreceptors

CGL thickness (μm)	*Dark decay* ($V s^{-1}$)	$E_{1/2}$ ($erg\,cm^{-2}$)		*Discharge at* $10\,erg\,cm^{-2}$ (%)
		$\lambda = 400$–$700\,nm$	$\lambda = 550\,nm$	
0·2	10	9·2	5·7	53
0·4	13	6·7	4·2	64

as the hole injection from CGL to CTL, cannot operate effectively in the photoreceptors with a PVK CTL. Compared with PVK, the hole mobility of TPD is two to three orders of magnitude higher and exhibits much less field dependence.[5] The mobility factor, however, is not prevailing in determining the difference between the two CTL materials. In summary, the higher carrier generation and hole injection efficiencies plus a secondary contribution from an improved hole mobility in CTL lead to a higher photosensitivity of perinone with TPD as CTL.

Extending the spectral response of bisarylimidazole perinone

Figure 12 shows the spectral response of dual-layer photoreceptors containing bisarylimidazole perinones **1**–**4**. The bis(2,3-naphthimidazole) perinone has substantially improved photosensitivity beyond 600 nm and actually extends to 700 nm. At 660 nm, $E_{1/2}$ is 6·6 erg cm^{-2} compared with 15 erg cm^{-2} for compounds **1**, **2** or **3**. Extending the aromaticity, as in compound **4**, extends the spectral response beyond 600 nm, but results in a decrease in the absorption peak monochromatic photosensitivity. A further device optimization study was carried out for **4** by increasing the CGL thickness from 0·2 to 0·4 μm. The results are summarized in Table 3 and indicate that a substantial improvement of photosensitivity can be obtained without causing high dark decay. The broad spectral response of bis(2,3-naphthimidazole) perinone and very flat response at 660 nm, where LED diodes emit, make this photogenerator particularly suitable for white light copier and LED printer applications.

REFERENCES

1. (a) Regensburger, P. J., *Photochem. Photobiol.*, **8** (1968) 429; (b) Regensburger, P. J. & Jakubowski, J. J., US Patent 3 879 200 (1975).

2. Loutfy, R. O., Kazmaier, P. M., Hor, A. & Burt, R., US Patent 4 808 506 (1989).
3. Wagner, H. J., Loutfy, R. O. & Hsiao, C. K., *J. Mat. Sci.*, **17** (1982) 2781.
4. Popovic, Z. D., Hor, A. M. & Loutfy, R. O., *Chem. Phys.*, **127** (1988) 451.
5. (a) Pai, D. M., *J. Non-Crystalline Solids*, **59–60** (1983) 1255; (b) Stolka, M., Yanus, J. F. & Pai, D. M., *J. Phys. Chem.*, **88** (1984) 4704.
6. Popovic, Z. D., private communication.